Texture Classification via Area-Scale Analysis of Raking Light Images

Andrew G. Klein
Dept. of Engineering and Design
Western Washington University
Bellingham, WA 98225
Contact email: andy.klein@wwu.edu

Anh H. Do and Christopher A. Brown
Dept. of Mechanical Engineering
Worcester Polytechnic Institute
Worcester, MA 01609

Philip Klausmeyer
Worcester Art Museum
55 Salisbury St.
Worcester, MA 01609

***Abstract*—An image processing algorithm for photographic and inkjet paper texture classification is developed based on area-scale fractal analysis. This analysis has been applied in surface metrology, and relies on the fact that the measured area of a surface depends on the scale of observation. By comparing relative areas at various scales, the technique computes a measure of the topological similarity of two surfaces. Results show the algorithm is successful in detecting affinities among similarity groupings within a dataset of silver gelatin photographic papers and a dataset of inkjet papers.**

I. Introduction

Being able to identify the manufacturer and type of paper on which a given photograph or inkjet print is made is a question of considerable interest to art historians and paper conservators. Knowledge of the specific type of paper used in a given print can assist with attribution and verifying authenticity when prints have uncertain provenance. Current approaches to photographic and inkjet paper identification rely on experts trained in paper conservation who inspect a variety of paper features such as the surface texture, thickness, and gloss. Due to the large number of different photographic and inkjet papers in existence, however, visually identifying the paper used for a given photographic print is an immense challenge, and automated or semi-automated approaches to photographic paper classification are desirable [1].

Recently, a reference collection of known silver gelatin photographic papers, all identified by manufacturer, brand, and date, has been assembled [2]. In parallel, a similar reference collection of inkjet papers has been assembled [3]. Digital photomicrographs of the surfaces of papers in both of these reference collections were acquired while using a "raking light", which is a linear light source at an oblique angle to the surface. The raking light is widely used by art conservators in the examination of art works since it enhances the highlights and shadows so that surface features are more clearly visible during image capture. The presence of these two reference databases of raking light images brings about the possibility of automated image-processing-based approaches: by comparing raking light images in the known database with those taken from a print made on unknown paper, it is possible that photographic and inkjet papers can be identified in an automated fashion.

As part of the Historic Photographic Paper Classification (HPPC) challenge [4], we and several other independent teams of researchers whose papers also appear in these conference proceedings [5]–[7] have developed image-processing-based approaches to perform automated paper classification. Several datasets of raking light images were assembled, consisting of a mix of known matches and known non-matches taken from both the Paul Messier Historic Photographic Papers Collection [2] and The Wilhelm Analog and Digital Color Print Materials Reference Collection [3], and these datasets were distributed to all teams for classification.

In this paper, we describe our specific technical approach to paper texture classification using raking light images, and we report on its performance when used to classify actual photographic and inkjet prints.

II. Technical Approach

A. Feature Extraction via Area-Scale Fractal Analysis

Image-processing-based texture classification is a topic which has seen a lot of research interest over the past several decades for use in a wide range of applications (see [8]–[10] and references therein for a survey of approaches). While the use of filter banks, wavelets, and textons have been quite popular in modern texture classification approaches for feature extraction (and indeed, several of the teams in the HPPC challenge

have adopted approaches based on wavelets [6] and textons [4]), we draw upon techniques from the field of surface metrology to leverage the unique features of raking light images. In particular, we rely on *area-scale fractal analysis* [11] which is a technique that has been applied to a diverse range of problems in surface metrology including, for example, analyzing the roughness of machined surfaces [12], characterizing food surfaces [13], and analyzing tooth wear in hominid fossils [14].

It is well-known that the measured *length* of a coastline depends on the scale of observation [15] since, as we zoom in, more detail is captured in the length measurement. Similarly, the measured *area* of a surface depends on the scale of observation. The area-scale approach [11] uses fractal analysis to decompose a surface into a patchwork of triangles of a varying sizes corresponding to varying scales of observation. Such a triangular patchwork decomposition of a surface is shown in Fig. 1, where the *nominal area* is the area of the flat portion projected underneath the surface, and the *measured area* is the sum of the areas of each of the triangles.

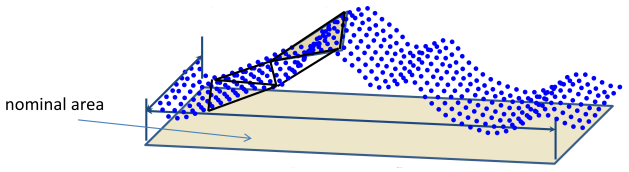

Fig. 1. Triangular Patchwork Decomposition of a Surface

As the size of the triangles in the patchwork is decreased (i.e. as we zoom in to finer scales), more surface features are captured in the measurement of the surface area. We define the *relative area* of a surface at a given observation scale as the ratio of the measured area divided by the nominal area, i.e.

$$\text{relative area} = \frac{\text{measured area}}{\text{nominal area}}. \tag{1}$$

Note that the nominal area does not change with the scale of observation, and relative area is always greater than or equal to 1. As the size of the triangles increases, smaller surface features become less resolvable and the relative area of the surface decreases, eventually approaching 1; an example of this effect is shown in Fig. 2.

Area-scale fractal analysis relies on the fact that the relative area versus scale of observation curve can be used to characterize a surface texture [12], [12]–[14].

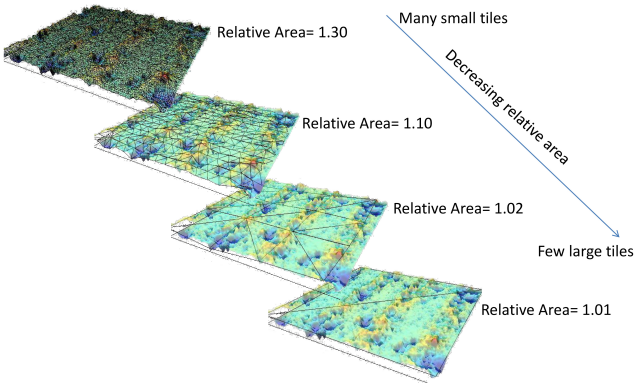

Fig. 2. Relative Area Decreases with Increasing Scale

As such, we consider the use of area-scale fractal analysis for feature extraction in the classification of paper textures.

B. Pseudo Area-Scale Applied to Raking Light Images

Area-scale fractal analysis relies on the availability of direct surface measurements, typically taken with a confocal laser scanning microscope (CLSM) or a scanning tunneling microscope (STM). Here, however, the provided datasets consist of microphotographs acquired with an optical microscope illuminated by a raking light [1], and direct surface measurements are not available. As such, we adopt greyscale illumination intensity as a proxy for surface height, by assuming that surface heights are roughly proportional to surface illumination. That is, we make the assumption that brighter greyscale intensities correspond to higher surface heights, while darker greyscale intensities correspond to lower surface heights.

The "scale" in this context is a measure of the size of the right triangles used for the triangular patchwork decomposition, and represents the length in pixels of each of the two non-hypotenuse sides of the triangles when projected into the 2-D plane (i.e. ignoring the "pseudo-height" of each pixel as given by the illumination). As such, at a scale of s, the 2-D projected patchwork consists of right triangles having sides equal in length to s pixels, so the length of the hypotenuse is equal to $\sqrt{2}s$ pixels, and the *nominal area* of a single triangle is equal to $\frac{1}{2}s^2$ square pixels. Because larger values of s correspond to "zooming out" or analyzing the image at coarser scales, the image effectively gets downsampled by larger and larger factors of s in both the horizontal and vertical direction as the scale increases. At a given scale s, there are s possible downsampling phases, yielding

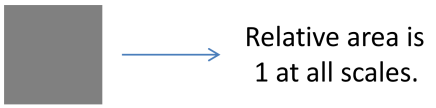

(a) Constant intensity

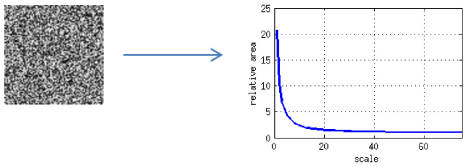

(b) Random i.i.d. intensities

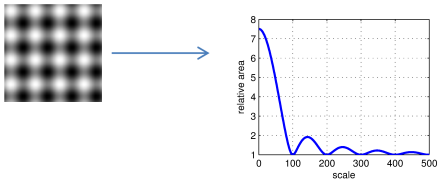

(c) Sum of two sinusoids (one in x, one in y)

Fig. 3. Example images and their relative area vs. scale curves

s different relative areas. As such, we average these s phases to use all of the information in the image.

Once the pseudo-height information is taken into account, the area of each triangle in the patchwork is larger due to "stretching" into the third dimension. If the three vertices of the first triangle in 3-D space are given by $(0, 0, h_1)$, $(0, s, h_2)$, and $(s, 0, h_3)$, for example, where these vertices have pseudo-heights (or greyscale intensities) h_1, h_2, and h_3, respectively, then the surface area of this triangle in 3-space can be shown to be

$$\frac{1}{2}s\sqrt{(h_1 - h_2)^2 + (h_1 - h_3)^2 + s^2}$$

which, again, has nominal area equal to $\frac{1}{2}s^2$ since the 2-D projected triangle has vertices $(0, 0)$, $(0, s)$, and $(s, 0)$. Using the greyscale illumination as a proxy for the height of each pixel, then, we can sum the measured areas of all of the decomposed triangular elements of the patchwork to compute the measured area, and ultimately the relative area from equation (1).

In Fig. 3 we show several synthetic but illustrative image surfaces, as well as the relative area versus scale curve for each of these surfaces. As expected, an image that has a constant intensity (i.e. when the texture is perfectly flat) has a relative area equal to 1 at all scales since the measured area always equals the nominal area. For a random i.i.d. surface which is highly faceted, the relative area is very high at small scales because all of the minute surface features are resolvable, whereas the image looks "flatter" at larger scales and eventually approaches a relative area of 1. In Fig. 3c we show the relative area versus scale curve for the sum of two sinusoids having period 100; in this case, we see that the relative area is 1 at every multiple of the period since the image looks perfectly flat when downsampled at scales s which are a multiple of the period.

These examples also demonstrate that the relative area as a function of scale is very different for different types of textures, and motivates area-scale fractal analysis as a choice for texture feature extraction. Since all textures have the property that the relative area approaches 1 as the scale grows significantly large, there is very little "information" at scales that exceed the size of the surface features in the underlying texture. Consequently, the choice of which scales are relevant for feature extraction depends heavily on the types of textures under investigation.

C. Summary of Approach

We now summarize the technical approach, including the algorithm parameters that were used, as well as the choice of distance metric. These parameters were determined through experimentation with the provided training dataset.

1) **Preprocessing**. All images were provided as 2080×1536 color images, representing 1.35×1.00 cm^2 of surface area. As a first step, we extract a 1024×1024 portion from the center, where the lighting is generally most consistent. Then, we convert the color image to greyscale and normalize the intensity to equalize the brightness of all images.
2) **Feature Extraction**. We perform area-scale fractal analysis on the preprocessed photomicrographs by using light intensity as a proxy for height. Through experimentation, we found that scales larger than 34 pixels (corresponding to lengths of 0.22mm) were not useful to classification since their inclusion did not change our results. We chose 8 logarithmically spaced scales between 1 and 34 pixels, which corresponded with the Fibonacci series, $\mathcal{S} = \{1, 2, 3, 5, 8, 13, 21, 34\}$. The 1024×1024 grid of equally spaced points (representing pixel locations) is decomposed into a patchwork of $2\left(\frac{N-1}{s}\right)^2$ isosceles right triangles at each scale $s \in \mathcal{S}$. The area of each triangle in 3-D space is then computed and the areas of all triangular regions are summed, resulting in the total relative area A_s at the chosen scale s. To conduct feature

extraction, then, the relative area for an image is computed over 8 scale values ranging from 1 pixel to 34 pixels, which correspond to lengths of 6.5 μm to 0.22 mm, respectively.

3) **Pairwise Distance Computation**. The topological similarity of two surfaces is computed by comparing the relative areas between two images at each scale. To classify and compare the similarity of two images i and j, a χ^2-distance measure $d(i,j)$ is computed via

$$d(i,j) = \sum_{s \in \mathcal{S}} \frac{\left(A_s^{(i)} - A_s^{(j)}\right)^2}{A_s^{(i)} + A_s^{(j)}}$$

where $A_s^{(i)}$ is the relative area of image i at scale s and $\mathcal{S}$ is the set of chosen scale values. Small values of $d(i,j)$ indicate high similarity between images i and j, while large values of d indicate low similarity.

The algorithm was written in Octave-compatible MATLAB code, and is freely available [16].

III. Numerical Results

A. Datasets

The first dataset consists of 120 *silver gelatin* photographic paper samples selected from [2]. The manufacturer, brand, texture, reflectance, and date have been catalogued by art conservators to serve as a reference benchmark. The dataset contains three levels of similarity: (1) samples from one same sheet (3 subsets of 10 samples), (2) samples from sheets taken from one same package (3 subsets of 10 samples); (3) samples from papers made to the same manufacturer specifications over a period of time (3 subsets of 10 samples). In addition, 30 sheets of interest to art conservators representing the diversity of silver gelatin photographic papers are included in the database. This dataset has been described in more detail in [1], [4] and is publicly available at papertextureid.org.

The second dataset consists of 120 *inkjet* paper samples selected from [3]. Again, the dataset contains the same three levels of similarity as described above (i.e. same sheet, same package, same manufacturing specifications), as well as a 30 additional diversity papers. This dataset has been described in more detail in [17].

B. Performance of Approach

Using the approach outlined in Section II-C, we processed the 120 images in each of the two datasets and generated pairwise distance metrics $d(i,j)$ for all possible pairs of images. For these results, the matrix of distance metrics was then converted to a grey-scale image with the darkest intensities indicating the greatest affinity and the lightest the least affinity.

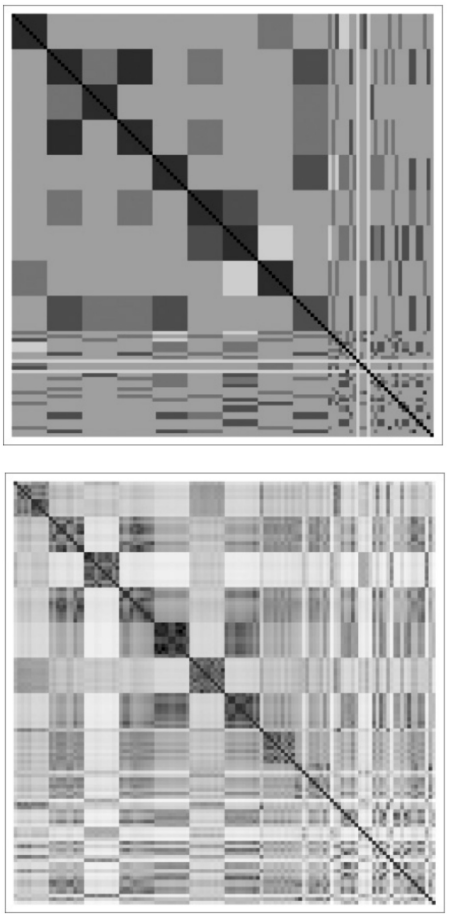

Fig. 4. Silver gelatin dataset results. Top: Known pairwise similarities, Bottom: Predicted pairwise similarities

The top of Fig. 4 shows known similarities for the silver gelatin dataset within the sample group suggested by the metadata including manufacturer, texture, brand, and date. As expected, the nine dark blocks starting in the upper left and continuing down along the diagonal show a high degree of affinity (dark gray and black) as these blocks depict the nine groups of similar textures. Lesser degrees of similarity are scattered throughout the figure with the 30 samples selected to show diversity (poorer levels of similarity) falling in the lower right quadrant and along the right side and bottom edge. The bottom of Fig. 4 shows the performance of our algorithm. The results largely coincide with the metadata and suggest that raking light photomicrographs have sufficient texture information to support the automated classification of historic photographic silver gelatin papers.

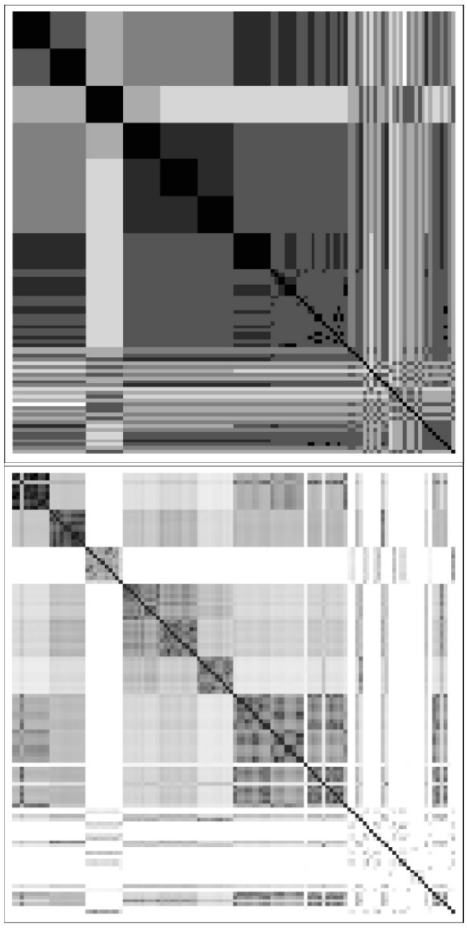

Fig. 5. Inkjet dataset results. Top: Known pairwise similarities, Bottom: Predicted pairwise similarities

Similarly, the top of Fig. 5 shows known similarities for the inkjet dataset within the sample group suggested by the metadata. Again, the nine dark blocks starting in the upper left and continuing down along the diagonal show a high degree of affinity, and again the results largely coincide with the metadata and suggest that raking light photomicrographs have sufficient texture information to support the automated classification of inkjet papers. In addition, the proposed results suggest the an area-scale approach yields good performance in classifying textures of photographic paper.

Future work will extend this approach to wove papers, and will investigate the connection between this triangular patchwork approach and existing wavelet-based schemes. The authors would like to thank Paul Messier, Henry Wilhelm, and the Museum of Modern Art (MoMA) for providing data for this project.

REFERENCES

[1] P. Messier and C. R. Johnson, Jr., "Texture feature extraction for the classification of photographic papers," in *Proc. Asilomar Conf. on Signals, Systems, and Computers*, Nov. 2014.

[2] P. Messier. (2014) The Paul Messier historic photographic papers collection. [Online]. Available: http://paulmessier.com/pm/collection.html

[3] H. Wilhelm, C. Brower, K. Armah, and B. Stahl. (2014) The Wilhelm analog and digital color print materials reference collection. [Online]. Available: http://www.wilhelm-research.com

[4] C. R. Johnson, Jr., P. Messier, W. Sethares, A. Klein *et al.*, "Pursuing automated classification of historic photographic papers from raking light photomicrographs," *Journal of the American Institute for Conservation*, no. 3, pp. 159–170, Aug. 2014.

[5] W. A. Sethares, A. Ingle, T. Krc, and S. Wood, "Eigentextures: An SVD approach to automated paper classification," in *Proc. Asilomar Conf. on Signals, Systems, and Computers*, Nov. 2014.

[6] P. Abry, S. Roux, H. Wendt, and S. Jaffard, "Hyperbolic wavelet transform for photographic paper texture characterization," in *Proc. Asilomar Conf. on Signals, Systems, and Computers*, Nov. 2014.

[7] D. Picard, S. Vu, and I. Fijalkow, "Second order model deviations of local Gabor features," in *Proc. Asilomar Conf. on Signals, Systems, and Computers*, Nov. 2014.

[8] J. Zhang and T. Tan, "Brief review of invariant texture analysis methods," *Pattern Recognition*, vol. 35, no. 3, pp. 735–747, 2002.

[9] M. Varma, "Statistical approaches to texture classification," Ph.D. dissertation, University of Oxford, 2004.

[10] T. Ojala, M. Pietikäinen, and D. Harwood, "A comparative study of texture measures with classification based on featured distributions," *Pattern recognition*, vol. 29, no. 1, pp. 51–59, 1996.

[11] C. A. Brown, P. D. Charles, W. A. Johnsen, and S. Chesters, "Fractal analysis of topographic data by the patchwork method," *Wear*, vol. 161, no. 1, pp. 61–67, 1993.

[12] C. A. Brown, W. A. Johnsen, R. M. Butland, and J. Bryan, "Scale-sensitive fractal analysis of turned surfaces," *CIRP Annals-Manufacturing Technology*, vol. 45, no. 1, pp. 515–518, 1996.

[13] F. Pedreschi, J. M. Aguilera, and C. A. Brown, "Characterization of food surfaces using scale-sensitive fractal analysis," *Journal of Food Process Engineering*, vol. 23, no. 2, pp. 127–143, 2000.

[14] R. S. Scott, P. S. Ungar, T. S. Bergstrom, C. A. Brown, F. E. Grine, M. F. Teaford, and A. Walker, "Dental microwear texture analysis shows within-species diet variability in fossil hominins," *Nature*, vol. 436, no. 7051, pp. 693–695, 2005.

[15] B. B. Mandelbrot, "How long is the coast of Britain?" *Science*, vol. 156, no. 3775, pp. 636–638, 1967.

[16] A. G. Klein and A. Do. (2014) Matlab source code for computing texture difference in papers. [Online]. Available: http://aspect.engr.wwu.edu/photopaper.m

[17] P. Messier, C. R. Johnson, Jr., H. Wilhelm, W. Sethares, A. Klein *et al.*, "Automated surface texture classification of inkjet and photographic media," in *Proc. Intl. Conf. on Digital Printing Technologies (NIP 29)*, Sep. 2013.